AIAA 80-1290R

Effect of Local Parameters on Gas Turbine Emissions

C. W. Kauffman,* S. M. Correa,† and N. J. Orozco†
University of Michigan, Ann Arbor, Mich.

The pollutant emissions from a gas turbine engine are affected by changes in local atmospheric conditions. Modeling efforts showed that these emissions also exhibit an extreme sensitivity to the details of the combustion process such as the local fuel-air ratio and the size of the drops in the fuel spray. Fuel-air ratios have been mapped under nonburning conditions using a single JT8D-17 combustor can at simulated idle conditions. Significant variations in the local values have been found. Modeling of the combustor employs a combination of perfectly stirred and plug flow reactors including a finite rate vaporization treatment of the fuel spray. Results show that a small increase in the mean drop size can lead to a large increase in hydrocarbon emissions and decreasing the value of the CO-OH rate constant can lead to large increases in the carbon monoxide emissions. These emissions may also be affected by the spray characteristics, with larger drops retarding the combustion process. Hydrocarbon, carbon monoxide, and oxides of nitrogen emissions calculated using the model accurately reflect measured emission variations caused by changing engine inlet conditions.

Nomenclature

c = specific heat of gas
C_D = drag coefficient
g = gravitational acceleration
k = thermal conductivity of gas
L = latent heat of vaporization
$\dot{m}_f$ = forced vaporization rate
$\dot{m}_s$ = static vaporization rate
Pr = Prandtl number
Q = heat of combustion
Re = Reynolds number
r = fuel-air ratio
t = time
V_a = air velocity
V_f = fuel drop velocity
V_{rel} = relative velocity
Y_O = oxygen concentration
ΔP = pressure drop across can
ΔP_N = pressure drop across nozzle
ΔT = difference between gas temperature and fuel boiling point
ρ_a = density of air
ρ_f = density of liquid

Introduction

THE emission levels from a gas turbine combustor are influenced by ambient conditions as well as by internal characteristics which include the spray vaporization, the mixing of the fuel and air, and the can aerodynamics. A series of experiments performed by Dils[1] shows peak-to-peak gas temperature oscillations from 200-2800°F within the combustor. These results suggest a lack of perfect mixing in the combustor and hence significant variation of the local fuel-air ratios. The experimental part of the work outlined here consists of a study of the mixing process as reflected in the local fuel-air ratio under nonburning conditions.

The effects of ambient conditions and the spray properties on the emissions were studied with a stirred reactor model. Osgerby[2] has categorized current models of gas turbine combustors as turbulent flame speed models, microvolume burning models, or stirred reactor models. Only the stirred reactor models are capable of predicting gross operating characteristics. Sophisticated computer programs are available which model the internal flowfield, the effects of turbulence and jet penetration, and the dynamics of the vaporizing fuel spray coupled with kinetic schemes of differing complexity.[3,4] These programs include several physical phenomena whose interactions are not completely understood. In this paper a less complicated approach is adopted. The stirred reactor models are well-suited to complex kinetic schemes and the results are easy to interpret. Although the choice of reactor volumes can be made at various levels of complexity, the stirred reactor model described here was kept straightforward so that the effect of ambient conditions and spray properties could be seen easily. This model combines finite-rate vaporization of the fuel spray with finite-rate chemistry to generate consistent temperatures and emissions without requiring large execution times.

The detailed local fuel-air data obtained experimentally has not been implemented in the stirred reactor model. This would call for a large number of reactors and an extrapolation of the cold-flow data to the burning situation with all the attendant uncertainties. Instead, the cylindrically symmetrical model formulated here allows for a direct study of the effect of drop size and ambient conditions on the predicted emissions.

Experimental Program

Test Apparatus

The experimental measurements were made in the test rig shown in Fig. 1, which accurately simulates idle conditions for a single JT8D-17 combustor can. The relevant parameters are $\dot{m} = 3.0$ lbm/s, $P = 2.5$ atm, $T = 250$°F and the fuel-air ratio is 0.0117. The air, which is supplied by a blowdown storage, is measured by a choked nozzle and is electrically heated. The diffuser section produces a uniform velocity profile, 65 ft/s, with a turbulence level of approximately 18%. The pressure in the test section is controlled by the addition of air at a choked orifice plate located downstream of the combustor.

As the test rig is cold-flow with no combustion occurring, the injection and vaporization of Jet A fuel would have been too slow to accurately represent the process in a burning combustor. Instead, indoline HO III as supplied by Amoco was substituted. It was heated within a heat exchanger to 250°F at a pressure of 500 psia. As verified by observation with a boroscope, the fuel quickly vaporized after injection.

The sampling system consists of a heated four-port probe and a port selector. The four ports are located at radial distances of $R = 0.25$, 1.0, 2.0, and 3.0 in. from the centerline with the first being designated as $R = 0$. The probe may be

Presented as Paper 80-1290 at the AIAA/SAE/ASME 16th Joint Propulsion Conference, Hartford, Conn., June 30-July 2, 1980; submitted Aug. 22, 1980; revision received June 11, 1981.

*Associate Research Scientist, Department of Aerospace Engineering. Member AIAA.
†Graduate Student, Department of Aerospace Engineering.

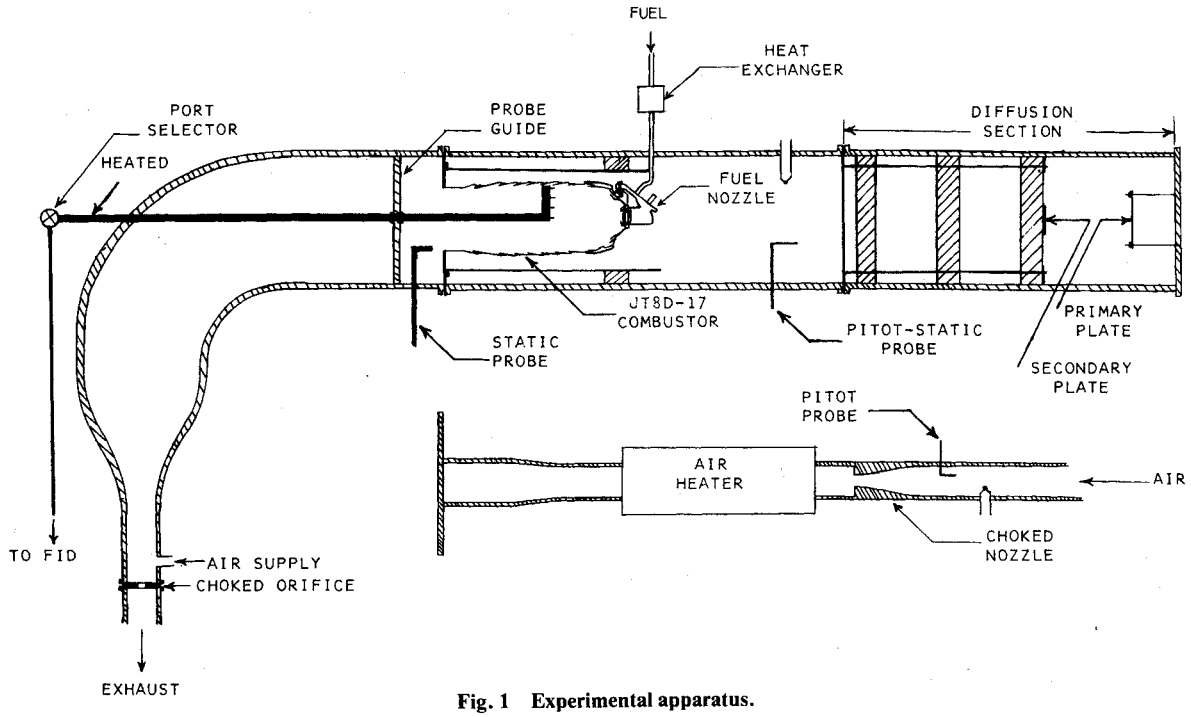

Fig. 1 Experimental apparatus.

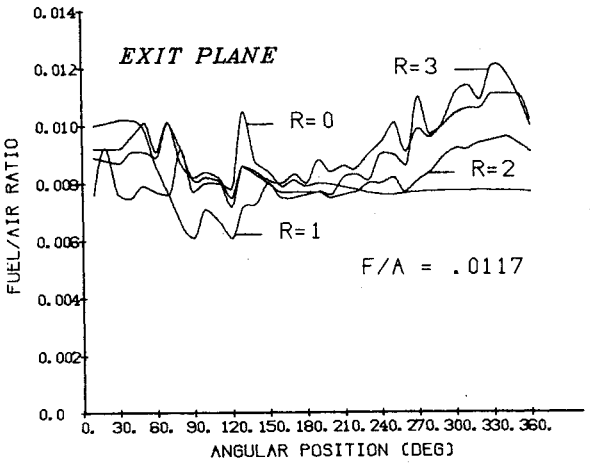

Fig. 2 Fuel-air ratio at exit plane.

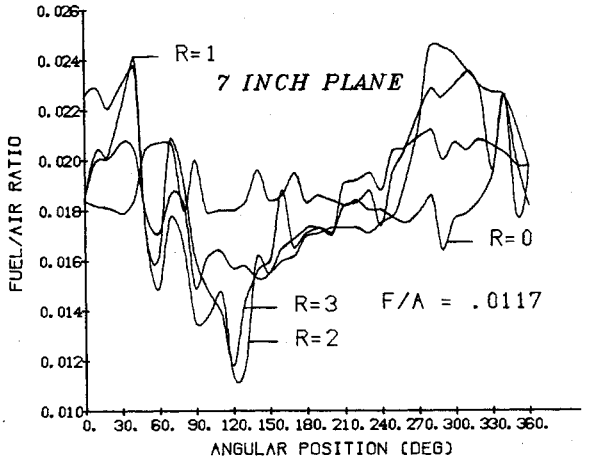

Fig. 3 Fuel-air ratio at 7-in. plane.

translated in the z direction along the axis of the combustor can and in the θ direction sweeping out each combustor plane. The fuel-air ratio of the sample was measured using a Scott flame ionization detector (FID) or a Lambda Scan equivalence ratio meter. The FID measured unburned hydrocarbons in a sample, and since hydrocarbons and air are the only constituents, the fuel-air ratio is easily calculated. The FID is only capable, however, of measuring a maximum of 100,000 ppm of hydrocarbons. The equivalence ratio meter was thus acquired so that measurements could be made well into the primary zone, where there is a higher concentration of fuel. Its operation is based on the measurements of residual oxygen concentration after a sample has been mixed with additional air and burned.[5]

Testing Methodology

The air and fuel flows were set and the probe was placed at a desired axial combustor location, with the exit plane being considered as the point of origin. Measurements were then made for each of the four radii at every 10 deg around the plane.

Experimental Results

Representative fuel-air ratio data are shown in Figs. 2-9. In Figs. 2-4 the value of the fuel-air ratio is given for the exit, 7-in., and 11-in. planes, for all four radii, and for all angular positions. At the exit plane the fuel-air ratio variation is minimal as, of course, is demanded by turbine inlet temperature uniformity considerations. However, as one moves upstream, variations in the fuel-air ratio become more severe even though the 7-in. plane is upstream of a major air inlet location. Generally speaking, as one would expect, the variations are least for small radii. The lack of cylindrical symmetry is perhaps somewhat surprising with variations in the fuel-air ratio of as much as 100% for a 10-deg azimuthal change. This effect is perhaps most clearly shown in the 5- and 9-in. planes (Figs. 5 and 6), where the fuel-air ratio has been averaged over the different radii. If this type of plot is examined for all planes one finds, for example, a consistent fuel deficit in the vicinity of 100 deg and a fuel surplus in the vicinity of 300 deg. Interpolation of the data for an entire plane gives results such as in Figs. 7-9. The height of the plot (at present unscaled) gives the fuel-air ratio and the azimuthal as well as the polar perspective is indicated. These plots ef-

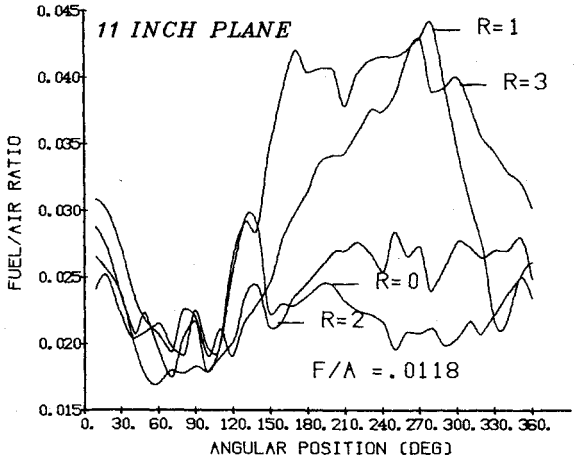

Fig. 4 Fuel-air ratio at 11-in. plane.

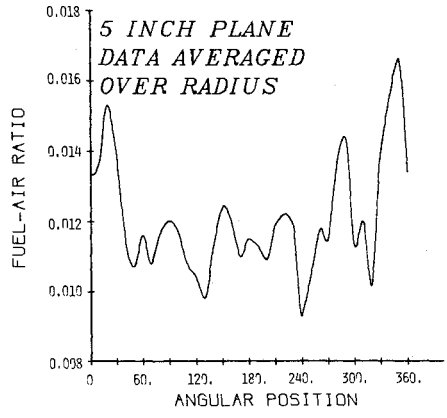

Fig. 5 Average fuel-air ratio at 5-in. plane.

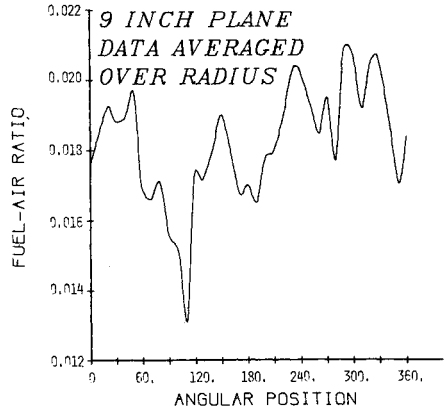

Fig. 6 Average fuel-air ratio at 9-in. plane.

fectively show the fuel-air ratio variation with perhaps a somewhat surprising uniform region near the edge. The data may be quantified as in Table 1. For each plane the average value of the fuel-air ratio has been calculated together with the standard deviation. If the standard deviation is normalized as in the last column, a meaningful comparison between planes is possible in that a large value of this quantity indicates larger variations in the fuel-air ratio. The three planes with the smallest values are the exit, 7-in., and 9-in. planes. The largest values of the parameter occur for planes located downstream of major dilution ports. The experimental measurements indeed seem to indicate that the fuel-air ratio within a combustor is far from uniform.

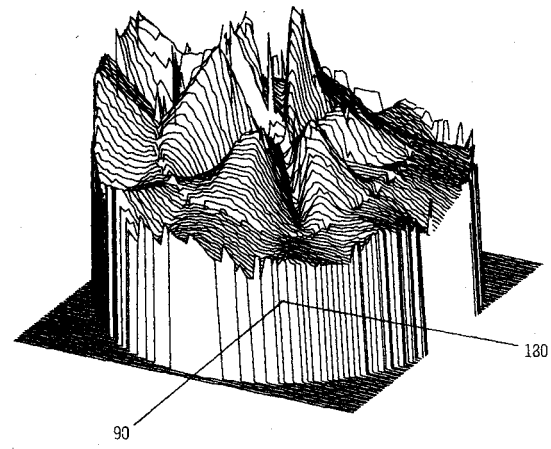

Fig. 7 Three-dimensional fuel-air ratio for 5-in. plane.

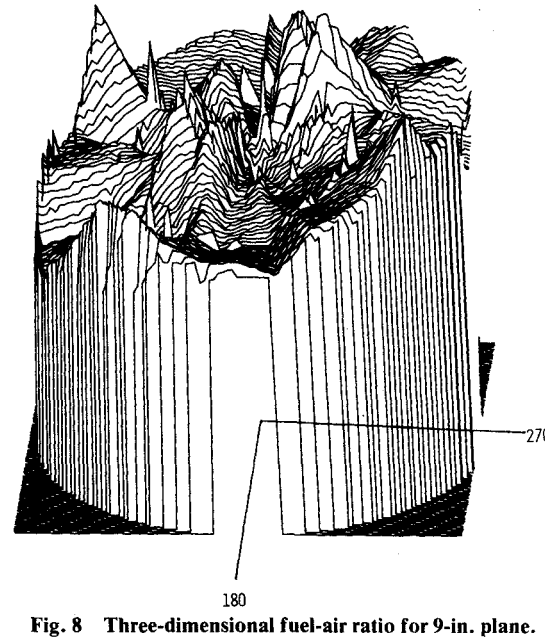

Fig. 8 Three-dimensional fuel-air ratio for 9-in. plane.

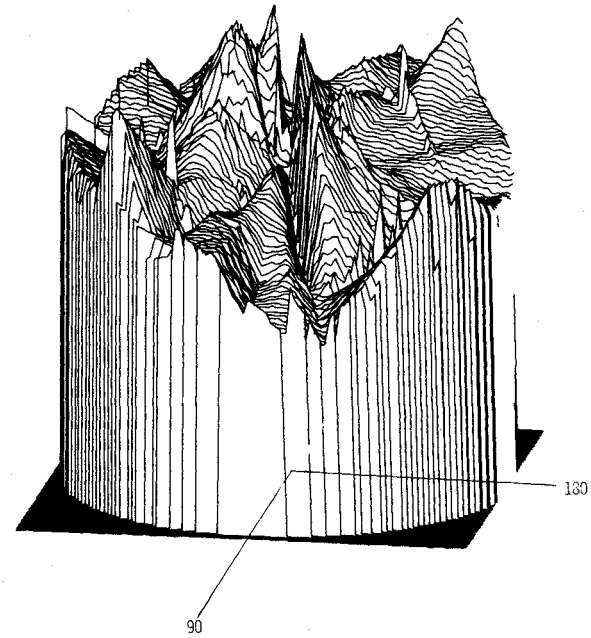

Fig. 9 Three-dimensional fuel-air ratio for 11-in. plane.

Analytical Effort

Emission Data

The goal of the analytical portion of this study is to predict emission levels of hydrocarbons (HC), carbon monoxide (CO), and oxides of nitrogen (NOx) as a function of changing ambient conditions for a JT8D-17 operating at idle thrust. Measured emission data previously obtained by Kauffman et al.[6] are given in Table 2 for a hot, dry day (120°F, 0% relative humidity), a hot, wet day (120°F, 100% relative humidity), and a cold, dry day (−20°F, 0% relative humidity). The results show that the hydrocarbon and carbon monoxide emission indices increase more rapidly with ambient humidity increases than with ambient temperature decreases, and that the oxides of nitrogen emission index decreases more rapidly with humidity increases than with temperature decreases. Also, as the fuel-air ratio increases, hydrocarbons and carbon monoxide decrease and the oxides of nitrogen increase.

The combustor inlet air flow is largest on the cold, dry day and least on the hot, wet day. Because the fuel-air ratio is a constant, the fuel flow rate has the same trend. If the primary fuel nozzle alone is operating, a higher fuel flow rate is the result of a larger pressure drop across the nozzle, which leads to improved atomization of the fuel, i.e., a smaller Sauter mean diameter (SMD). The SMD is thus expected to be largest on the hot, wet day and smallest on the cold, dry day. Simultaneous fuel flow in the primary and secondary nozzle is more difficult to characterize, so the bulk of the analytical work has been done for a pressure ratio of 2, as then only the primary nozzle was in operation.

Vaporization Model

Hydrocarbon emissions may be calculated by considering the vaporization of fuel drops as they pass through a high temperature environment matching that within a combustor. The process of the evaporization of a fuel spray was carefully detailed by Marchionna.[7] The static vaporization rate for a drop of diameter D

$$\dot{m}_s = \frac{2\pi kD}{c} \ell n \left[1 + rY_O \left(1 + \frac{Q}{L} \right) + \frac{c\Delta T}{L} \right]$$

is enhanced by the droplet injection velocity according to

$$\dot{m}_f = \dot{m}_s (1 + 0.276 Re^{0.5} Pr^{0.33})$$

Table 1 Average and standard deviation of the fuel-air ratio

Plane	Average fuel-air ratio, f/a	Standard deviation, σ	$\frac{\sigma}{f/a}$
Exit	0.0089	0.0012	13.8
5	0.0122	0.0029	24.0
7	0.0182	0.0027	14.2
9	0.0182	0.0023	15.4
11	0.0230	0.0072	26.6
13	0.0457	0.0100	21.9

where for burning conditions $Pr = 0.7$. The initial relative velocity between the drop and the air in the combustor is given by

$$V_{\text{rel}}^2 = V_a^2 + V_f^2$$

where

$$V_f^2 = c_1 g \Delta P_N / \rho_f$$

and

$$V_a^2 = c_2 g \Delta P / \rho_a$$

c_1 and c_2 being empirical constants. The relative velocity of course decreases owing to drag forces on the drop and is given by

$$\frac{dV_{\text{rel}}}{dt} = \frac{3}{4} \frac{C_D}{D} \frac{\rho_a V_{\text{rel}}^2}{\rho_f}$$

where

$$C_D = \frac{28}{Re^{0.85}} + 0.48$$

The spray is modeled as a Rosin-Rammler distribution, but the exact distribution could be used if available. The size range is divided into 21 groups, each represented by its median diameter. The vaporization rate is computed for each group and is assumed to be constant for 0.1 ms. The pertinent variables in the vaporization equations are then updated. This process is continued for the residence time period in a particular combustor zone or until all the mass in the particular size group has been vaporized. The vaporized part of the spray is considered to be available for the combustion process.

The vaporization model gives realistic hydrocarbon emissions when proper conditions within each combustor zone are specified. In this as yet incomplete model the conditions must be calculated separately or estimated. Figure 10 shows the effect of ambient conditions on hydrocarbon emissions. If realistic SMD's are estimated as indicated on the plot, the hydrocarbon emissions follow the trend in Table 2. The emission sensitivity to drop size is in good agreement with hydrocarbon emission data obtained by Buchheim.[8]

Bragg Combustor

The Bragg combustor is a gas-phase-only simulation of a gas turbine combustor using idealized reactors. The primary zone is represented by a perfectly stirred reactor (PSR) and the secondary and dilution zones are represented by plug flow reactors (PFR). In the PSR both axial and lateral mixing are allowed, accounting for primary zone recirculation, while in the PFR only lateral mixing is allowed. A full kinetic scheme is employed in order to predict the carbon monoxide and oxides of nitrogen emissions. There are, of course, practically no hydrocarbon emissions. The computational code upon which the model is based, CREK, was originally developed by Pratt and Wormeck.[9]

Table 2 Experimental emission data

	Pressure ratio = 2					
	$f/a = 0.011$			$f/a = 0.015$		
	120°F $RH=0$	120°F $RH=1$	−20°F $RH=0$	120°F $RH=0$	120°F $RH=1$	−20°F $RH=0$
EI-HC	28.0	75.0	46.0	12.0	40.0	25.0
CO	87.0	135.0	115.0	65.0	105.0	95.0
NO	0.9	0.5	0.6	1.1	0.5	0.7
NOx	2.2	0.8	1.4	2.5	0.8	1.5

For this model the airflow schedule and reactor volumes are given in Fig. 11. This simulates the JT8D-17 at idle. The fuel is assumed to be prevaporized and introduced in the primary zone. Initial runs with this model employing reactions 1-17 of the kinetic scheme in Table 3 gave unrealistically low carbon monoxide emissions. Figure 12 shows how the predicted carbon monoxide index depends upon the rate constant for reaction 2 ($CO + OH = CO_2 + H$). As the measured emission indices are of the order of 10-100, a preexponential rate constant of $10^{5.65}$ was employed in further calculations. This rate constant is lower than the values available in the literature; however, there is considerable doubt as to whether this is really an Arrhenius-type reaction, so that the available kinetic data becomes difficult to use. It is also known that carbon monoxide emissions are controlled by the oxidation rate in the secondary and dilution zones rather than by the production rate in the primary zone. As might be expected, an increase in the rate constant for reaction 1 was found to have little effect on increasing the carbon monoxide emissions. As Table 4 shows, the Bragg combustor is capable of predicting some results which are of the proper magnitude and trends even at high power conditions.

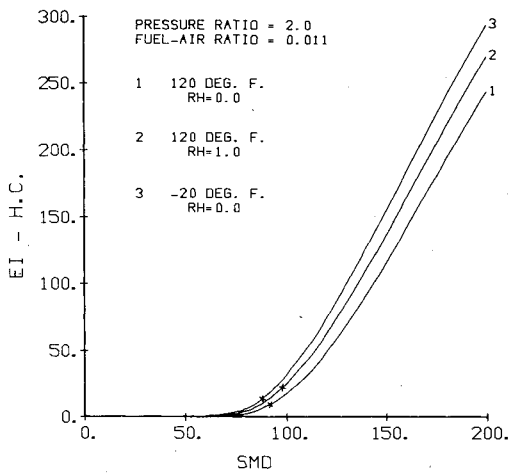

Fig. 10 Effect of ambient conditions on vaporization model.

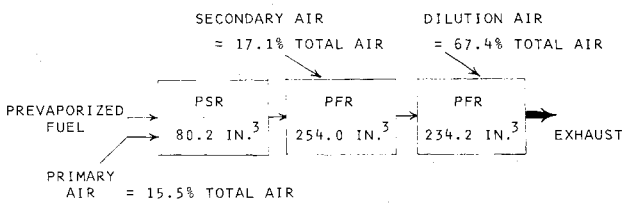

Fig. 11 Bragg combustor model.

Coupled Model

In this model vaporization and kinetics have been combined. The amount of vaporization of the fuel drops determines the fuel-air ratio and thus the temperature, which then determines the amount of drop vaporization. The iteration scheme for the coupled model, based upon temperature, is shown in Fig. 13. The previously described computational schemes are employed for the vaporization and kinetic calculations. In the limit of small SMD's, the Bragg combustor results are reproduced.

For the JT8D-17 the compressor discharge conditions for different engine inlet conditions may be accurately calculated and the air distribution pattern for the combustor has been

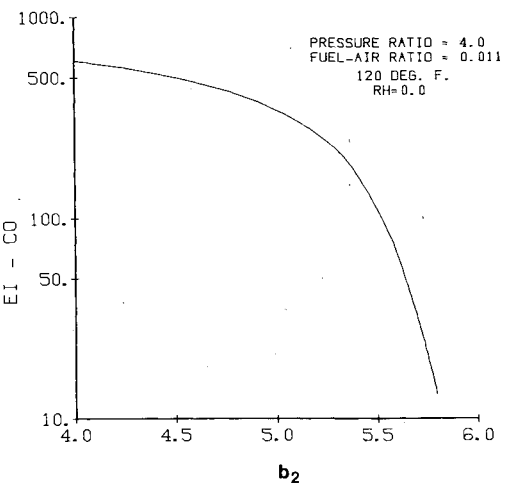

Fig. 12 Effect of rate constant on carbon monoxide emissions.

Table 3 Kinetic scheme (SI units)

						Forward rate constant $k_j = 10^{b_j} T^{n_j} \exp(-T_j/T)$		
						b_j	n_j	T_j
1	C_8H_{16}	O_2	$\bullet = CO$	H_2	$\bullet$	8.500	0.0	12,200.0
2	CO	OH	$\bullet = CO_2$	H	$\bullet$	6.600	0.5	0.0
3	CO_2	$\bullet$	$M = CO$	O	M	12.000	0.0	50,353.0
4	H	OH	$\bullet = H_2$	O	$\bullet$	6.903	1.0	3,525.0
5	H_2O	$\bullet$	$M = OH$	H	M	12.477	0.0	52,870.0
6	H	HO_2	$\bullet = OH$	OH	$\bullet$	11.398	0.0	957.0
7	OH	H_2	$\bullet = H$	H_2O	$\bullet$	10.398	0.0	2,618.0
8	H	O	$M = OH$	$\bullet$	M	9.903	0.0	0.0
9	OH	O	$\bullet = H$	O_2	$\bullet$	10.398	0.0	0.0
10	H	O_2	$M = HO_2$	$\bullet$	M	9.176	0.0	503.5
11	OH	OH	$\bullet = H_2O$	O	$\bullet$	9.778	0.0	503.5
12	OH	N	$\bullet = H$	NO	$\bullet$	8.778	0.5	4,028.0
13	H	N_2O	$\bullet = OH$	N_2	$\bullet$	10.903	0.0	7,553.0
14	N	NO	$\bullet = N_2$	O	$\bullet$	10.176	0.0	0.0
15	N	O_2	$\bullet = NO$	O	$\bullet$	6.778	1.0	3,172.0
16	N_2O	O	$\bullet = NO$	NO	$\bullet$	11.000	0.0	15,000.0
17	N_2O	$\bullet$	$M = N_2$	O	M	11.000	0.0	25,176.0
18	NO	HO_2	$\bullet = NO_2$	OH	$\bullet$	5.480	1.0	0.0
19	NO_2	H	$\bullet = NO$	OH	$\bullet$	11.860	0.0	971.0
20	NO_2	O	$\bullet = NO$	O_2	$\bullet$	10.000	0.0	302.0
21	CN	H_2	$\bullet = HCN$	H	$\bullet$	10.780	0.0	2,667.0
22	HCN	O	$\bullet = CN$	OH	$\bullet$	8.150	0.68	8,505.0

Table 4 Bragg combustor results

Ambient conditions	Idle conditions ($PR=2; f/a=0.011$) R1-R20, $b_1=8.50$, $b_2=5.65$ 120°F $RH=0$	120°F $RH=1$	−20°F $RH=0$
EI-CO	230.3	176.6	293.1
EI-NO	1.209	0.187	0.640
EI-NO_2	0.207	0.033	0.114
EI-NOx	1.416	0.220	0.754

Takeoff conditions ($PR=17.4, f/a=0.0182$)

	Measured	Calculated
EI-CO	0.55	1.38
EI-NOx	24.4	10.4

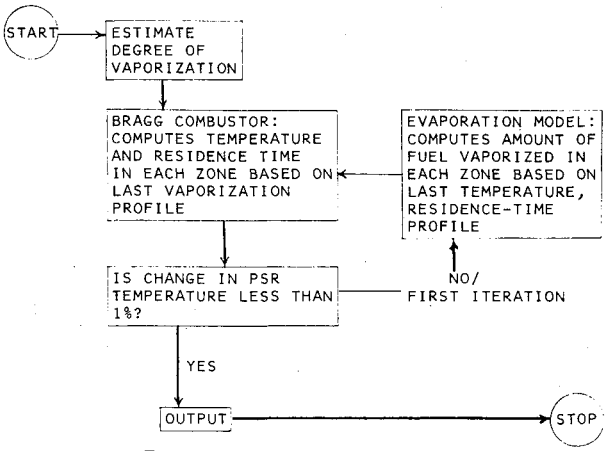

Fig. 13 Coupled combustor model.

accurately measured. However, data relating to the fuel spray characteristics are not extensive. Hence it has been necessary to conduct the calculations treating the SMD as a variable. The SMD's may be estimated using an appropriate relationship and the corresponding emissions may then be obtained. This approach shows the sensitivity of emissions to the mean drop size.

Figures 14-16 show the emission indices calculated for a fuel-air ratio of 0.015 using reactions 1-17 of the kinetic scheme. Using the values of SMD's indicated on the figures gives the proper trends with ambient conditions for the hydrocarbon and carbon monoxide emission indices. The nitric oxide emission index shows the proper trend regardless of the SMD. For a fuel-air ratio of 0.015 the primary zone is rich. As increasing the SMD decreases the rate of vaporization, the primary zone is driven toward stoichiometric with an attendant increase in temperature clearly leading to an increase in the nitric oxide and ultimately to additional carbon monoxide. Such a trend has been experimentally measured by Buchheim[8] for the regenerative automotive gas turbine. It is also significant that the 50-60-μ "barrier," only above which the emissions are affected by the vaporization process, is also apparent from Buchheim's results.

Figures 17-19 show the emission indices for an overall fuel-air ratio of 0.011, again using reactions 1-17. In this situation the primary zone is near stoichiometric and the effect of retarded vaporization is to make it leaner, thus decreasing the flame temperature. The nitric oxide emissions are thereby lowered and the carbon monoxide emissions also decrease. If realistic SMD's are chosen again, the hydrocarbon and nitric oxide emission indices show the proper trend while the carbon monoxide emission index on the hot, wet day is always too low.

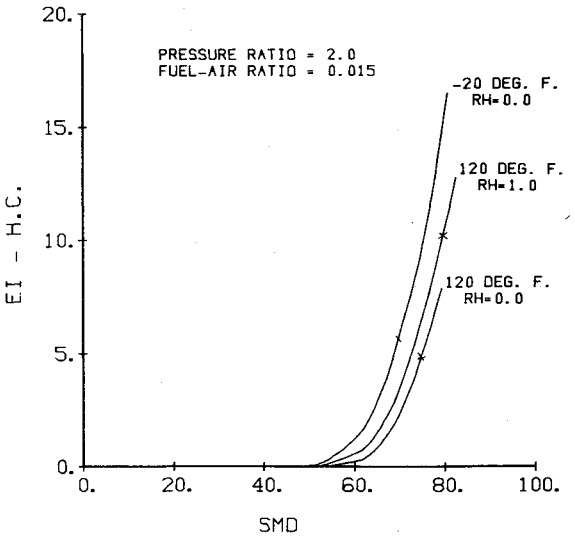

Fig. 14 Hydrocarbon emissions—17 step scheme.

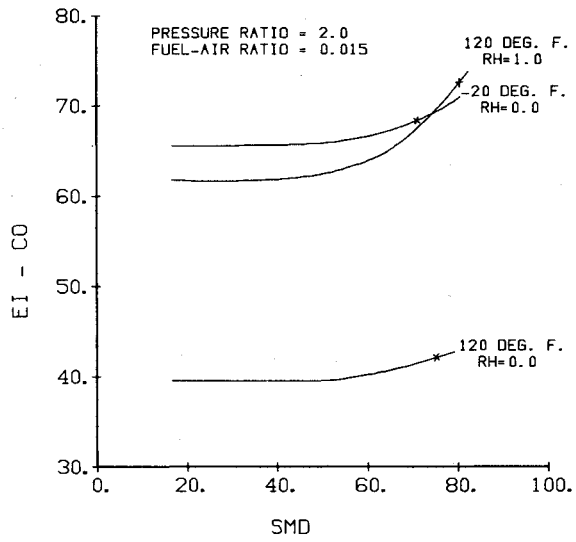

Fig. 15 Carbon monoxide emissions—17 step scheme.

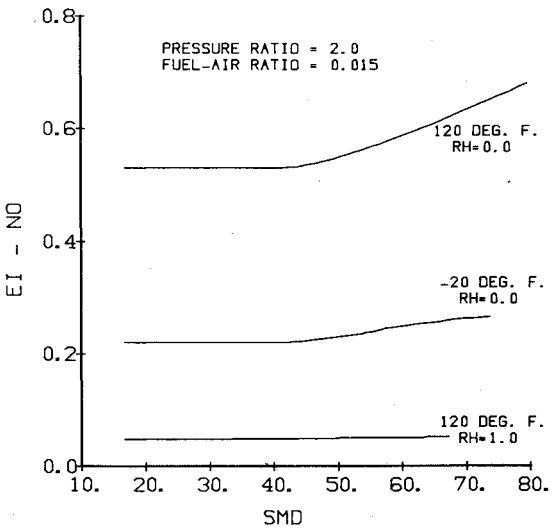

Fig. 16 Nitric oxide emissions—17 step scheme.

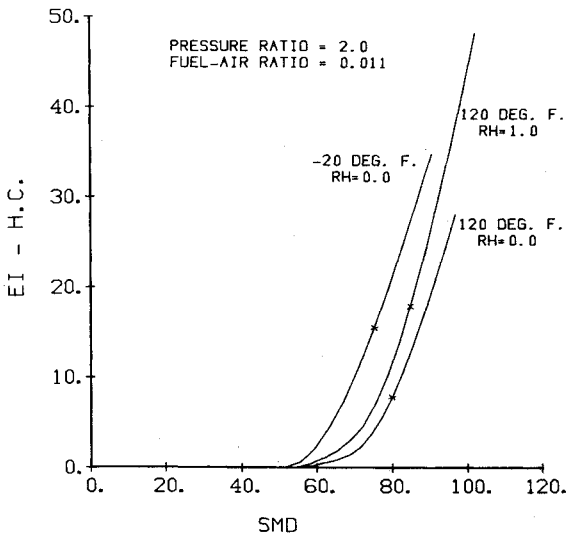

Fig. 17 Hydrocarbon emissions—17 step scheme.

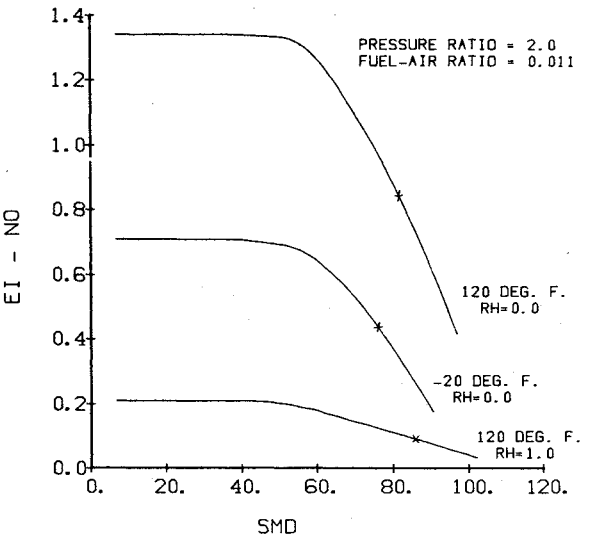

Fig. 19 Nitric oxide emissions—17 step scheme.

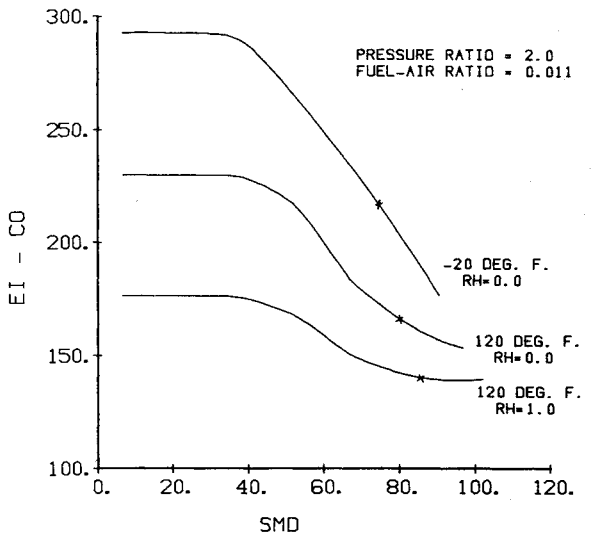

Fig. 18 Carbon monoxide emissions—17 step scheme.

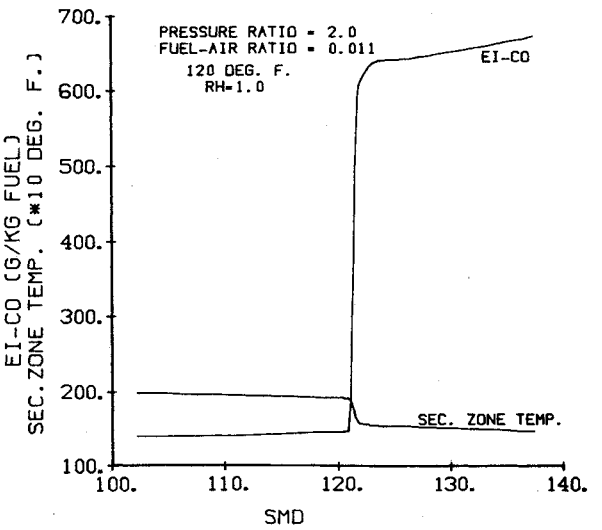

Fig. 20 Carbon monoxide emissions—large fuel drops.

As the experimental data showed that a considerable quantity of nitrogen dioxide was present in the oxides of nitrogen, the kinetic scheme was expanded in an attempt to account for its production. Emissions were calculated for a fuel-air ratio of 0.015 using reactions 1-22 in the kinetic scheme. For these conditions the nitrogen dioxide can be made to account for approximately 20% of the oxides of nitrogen while it was measured to be near 50%. The results were in general agreement with those of Figs. 15-17 except for the carbon monoxide, which was too low on the hot, wet day.

If the calculations are extended to larger SMD's, the coupled model predicts an abrupt increase in the carbon monoxide emission index, as seen in Fig. 20. This corresponds to the extinction of the flame in the secondary zone because of the failure of the drops to evaporate. The iterative scheme converges to a nonburning solution. Although the change occurs quite rapidly with SMD, the addition of inhomogeneities within the combustor would produce a lesser gradient, as apparent from Buchheim's measurements.

Under leaner conditions of a fuel-air ratio of 0.007, the PSR in the coupled model does not ignite for the cold and wet days unless smaller drops are chosen or the rate constant k_1 is increased. The slow rate of vaporization lowers the PSR equivalence ratio below the flammability limit. If the primary zone is modeled as a smaller PSR followed by a PFR—the total volumes of which equal the original PSR—as the PSR volume is decreased ignition will occur. However, at present, emissions computed under these conditions do not reflect the experimental data.

Table 5 Preliminary results of the new model[a]

Condition ($PR=2, f/a=0.015$, cold dry day) R1-R20, $b_1=8.5, b_2=6.6$	EI-HC	EI-CO	EI-NO	EI-NO_2
New model	7.2	3.91	0.36	0.15
Coupled model	24.9	29.77	0.43	0.15
Experiment	25.0	95.0	0.70	0.80

[a] In the new model: core radius is 93.5% of can radius; 5% PSR exhaust feeds into liner; 20% of secondary, dilution air feeds into liner.

Liner Model

The carbon monoxide concentration in an actual combustor is observed to peak in the wall region as, for example, shown by the measurements of Wolters.[10] Its oxidation rate is reduced here because of the lowered local temperature. Through the use of nonhomogeneous regions in the combustor, it is possible to use a rate constant for reaction 2 which is larger and in better agreement with that in the literature.

The coupled model has been modified to allow the PSR exhaust to feed into a thin, lean liner region and a large, richer core region. At present, the PSR exhaust diversion, the secondary and dilution air diversion, and the liner and core reactor volumes are input to the model. These quantities are clearly related to can aerodynamics. Reasonable estimates for these quantities do, however, yield realistic levels of carbon monoxide, as shown in Table 5. Models could be formulated with several streamtubes in parallel, thereby allowing for highly nonuniform fuel-air ratios and any prescribed heat transfer rate to the liner. However, the model presented here has been kept simple so that the cause-effect relationships between ambient conditions, spray parameters, and emissions are obvious.

Conclusions

Measurements of the local fuel-air ratios within a JT8D-17 combustor under nonburning conditions show a high degree of nonuniformity which could affect the emissions significantly. The magnitudes and trends of emissions with varying ambient conditions have been reasonably predicted using a finite-vaporization-rate stirred reactor model. The model shows that the fuel spray atomization characteristics significantly affect the emissions. Better experimental data are required relating to the spray characterization, combustor can aerodynamics, and the behavior of the primary zone under lean combustion conditions.

Acknowledgments

The authors would like to express their appreciation to N. Marchionna of Avco Lycoming and D. T. Pratt of The University of Michigan for generously making available copies of their computer programs. The efforts of J. Draxler in obtaining the experimental data were also significant. The work was supported under NASA Grant NSG 3165, NASA Lewis Research Center, Airbreathing Engines Division, David Ercegovic, Contract Monitor.

References

[1] Dils, R.R., "Dynamic Gas Temperature Measurements in a Gas Turbine Transition Duct Exit," *Journal of Engineering for Power,* Vol. 95, July 1973, Series A, No. 3, pp. 265-277.

[2] Osgerby, I.T., "Literature Review of Turbine Combustor Modeling and Emissions," *AIAA Journal,* Vol. 12, June 1974, pp. 743-754.

[3] Mosier, S.A. and Roberts, R., "Low-Power Turbopropulsion Combustor Exhaust Emissions," Pratt and Whitney Aircraft Tech. Rept. AFAPL-TR-73-36, July 1973.

[4] Bruce, T.W., Mongia, H.C., and Reynolds, R.S., "Combustor Design Criteria Validation," AiResearch Manufacturing Company of Arizona, USARTL-TR-78-55A, March 1979.

[5] Haslett, R.A and Eidson, T.M., "Equivalence Ratio Meter," SAE Paper 770219, *SAE Congress and Exposition,* Cobo Hall, Detroit, Mich., Feb.-March 1977.

[6] Kauffman, C.W., Subramaniam, A.K., Rogers, D.W., and Claus, R.W., "The Effect of Ambient Conditions on the Emissions of an Idling Gas Turbine," AIAA Paper 78-3, Jan. 1978.

[7] Marchionna, N., Watkins, S., and Opdyke, G., "Turbine Fuel Tolerance Study," Avco Lycoming, TACOM Rept. 12090, Oct. 1975.

[8] Buchheim, R., "Untersuchungen zum Emissions verhalten von Pkw-Gasturbinenbrennkammern," Technischen Hochschule Aachen, March 1977.

[9] Pratt, D.T. and Wormeck, J.J., "CREK: A Computer Program for Calculation of Combustion Reaction Equilibrium and Kinetics in Laminar or Turbulent Flow," Rept. WSU-ME-TEL-76-1, Washington State University, Pullman, Wash., March 1976.

[10] Wolters, H.R., "Experimenteel onderzoek naar het verbrandings verloop in een gasturbine verbrandingrkramer en de invloed van water-injectie op de volumuna van stikstofoxiden," Technische Hogeschool, Delft, March 1973.